ESTIMATING DOSIMETRIC QUANTITIES OF RADON PROGENY USING HUMAN CT SCAN DATA AND SMALL TISSUE VOLUME ANALYSIS WITH Geant4 CODE SYSTEM

by

Evelynn VAN DEN AKKER, Matthew LUND, and Tatjana JEVREMOVIC*

Nuclear Engineering Program, The University of Utah, Salt Lake City, Ut., USA

Scientific paper
DOI: 10.2298/NTRP1503203A

Estimating the health effects of radon exposure is of great interest because radon is considered the second leading cause of lung cancer after smoking. The dose-response curve is not well understood at low-dose levels where radon exposure is estimated. Therefore, the health mechanisms of radiation due to radon progeny at the cellular and molecular levels are of interest for providing an indication of a possible threshold value above which the exposure may indicate cancer formation. In this paper we present a macroscopic and cellular level numerical analysis of the radon-induced dose estimates based on the Geant4 code system. Macroscopic estimates are assessed based on patient-specific computer tomography scans that provide geometries easily applicable to modeling radiation effects of the radon progeny sources. A small tissue volumes analysis based on the Geant4 code system is developed so as to provide information about the interactions and particle track structures at the microscopic (cellular) levels producing the dosimetric effects of radon short-lived progenies. The results presented in this paper also call attention to the capabilities of Geant4 to provide radon-related dosimetric parameters of large and small-scale biological systems.

Key words: dosimetry, radon, Geant4, computed tomography

INTRODUCTION

Radon is considered to be the second leading cause of lung cancer after smoking [1]. It can be found in high concentrations indoors, worldwide. Epidemiological studies have attempted to quantify the risks associated with prolonged exposures. Studies have found a correlation between low-dose radon exposure and lung cancer mortality and assigned an excess relative risk of 11 % increase in mortality for every 100 Bq/m^3 increase in indoor radon concentration [1]. Agencies such as the environmental protection agency (EPA) and the world health organization (WHO) have based their recommendations for remediation levels of radon concentration on the linear no-threshold (LNT) dose-response model put forth by epidemiological studies. The assumption is that just one alpha particle can cause DNA damage that would lead to the formation of cancer. There are, however, conflicting studies on the validity of the LNT dose-response model and the 2013 MELODI Committee called for more research on the nano-scale levels with the goal of identifying the interactions and biological responses that lead to DNA damage, cell mutation, and neoplastic formation [2].

* Corresponding author; e-mail: tatjana@chemeng.utah.edu

In this paper we show a simulation model based on the particle tracking code Geant4 in modeling macroscopic and microscopic effects of radon exposure. The macroscopic model is based on patient-specific geometry from computed tomography (CT) scans; the effect is related to the estimate of dose rates in the lungs resulting from the decay of short-lived radon progeny. Additionally, the interactions from the decay products in small target tissue volumes are analyzed using the Geant4-DNA toolkit in estimating the microscopic effects of radon exposure. The ionization events of alpha particles interacting with the cell nucleus are the main mechanisms by which the radiation induces double-strand breaks in the DNA molecule, whether through direct interactions or hydrolysis and the release of radicals in the vicinity of the DNA molecule [3].

METHODS AND MATERIALS

Radon exposure

^{222}Rn is a significant source of low-dose ionizing radiation that contributes to a majority of a person's annual background dose. The ^{238}U decay chain is de-

Table 1. ^{238}U decay chain with ^{222}Rd short-lived progency [4]

^{238}U decay chain	Half-life	Main decay path
^{238}U	4.5 10^6 year	α
^{234}Th	24.1 d	β
^{234}Pa	1.159 min	β
^{234}U	2.4 10^5 year	α
^{230}Th	7.5 10^4 year	α
^{226}Ra	1600 year	α
^{222}Rn	3.8 d	α
^{218}Po	3.1 min	α
^{214}Pb	26.8 min	β
^{214}Bi	19.9 min	β
^{214}Po	164 s	α
^{210}Pb	22.2 year	β
^{210}Bi	5.0 d	β
^{210}Po	138.4 d	α
^{206}Pb	Stable	–

tailed in tab. 1 [4], with the short-lived radon progeny also shown. The gaseous, chemically inert radon readily becomes airborne, but on its own poses little threat in typical activity concentrations, because it does not collect or deposit in the body. The particulate decay products are likely to attach to molecules in the air (usually indicated as the attached fraction) or a smaller portion may remain free of surrounding particles (called the unattached fraction) [5, 6]. A larger portion of these decay products deposit in the main bronchial bifurcation and, due to their relatively short half-lives, decay where they are deposited [5, 6]. Alpha radiation from the ^{218}Po and ^{214}Po delivers the majority of the dose due to its short-range in tissue. Beta and gamma emissions contribute significantly less to the cumulative radiation dose and are often neglected when estimating the overall radon effects.

There are two other radon isotopes: ^{220}Rn (thoron) and ^{219}Rn (actinon). Their gaseous form might give them the chance to collect in homes, but their half-lives are so short (56 s and 4 s, respectively) compared to ^{222}Rn that their chance of decaying before escaping their matrix formation and becoming airborne is much greater [5]. Thus, contributions of thoron and action progenies to the human lung dose are usually neglected.

Currently, lung cancer risk estimates for occupational and residential radon exposures are based on epidemiological studies of miners. Lung cancer mortality is correlated with exposure to radon progeny in miners, typically working in conditions that do not qualify as low-dose exposure. The results of these studies were then extrapolated to those whose exposure is residential and categorized as low-dose. Uncertainty accompanies every measurement or calculation, but is often absent when these epidemiological data are used for residential radon exposure risk assessment. The Biological Effects of Ionizing Radiation, BEIR VI, report addressed these issues indicating that data on individual exposures were not well-defined interims of the spatial variation of radon concentrations, time spent in different zones, and various other parameters related to individual workloads, respirator use, and different professions [7].The report also signaled the problem of accurate recording exposures in mines where data was suppressed if it was outside the established safety limits. The report indicates that, as far as these studies are concerned, the uncertainties amounted to "hundreds of percent" and, consequently, put into question all of the risk estimates based on them.

There is, therefore, a clear need to minimize the risk of cancer mortality due to random radon exposure and to identify levels at which the indoor radon concentration poses a less or equal risk to the acceptable one. The largest challenge facing researchers is to define the dose-response relationship at low doses. A comprehensive review of available biological and biophysical data supports a LNT risk model which predicts that the risk of cancer proceeds in a linear fashion at lower doses without a threshold and that the smallest dose has the potential to cause a small increase in risk to humans [8]. Cohort studies of miners working in high-to-moderate dose level environments provide a framework from which to extrapolate the excess relative risk (ERR) at low-dose residential concentrations. The association between radon and lung cancer risk have been examined in large-scale studies and pooled studies to determine how increasing radon concentrations are related to lung cancer mortality.The bulk of literature agrees that radon exposure correlates to lung cancer and that there is an ERR of about 15 % for each 100 Bq/m^3 increase in radon concentration [1]. These studies support the LNT dose-response model which states that exposure to ionizing radiation and risk of cell mutation and neoplastic transformation are linearly related [9]. Furthermore, the Committee on the BEIR VII report has also supported these findings, citing the availability of new and more extensive data which have strengthened confidence in the estimates [7]. Since the shape of the dose-response curve at low doses is not well understood, the risks estimated by the epidemiological studies are also not well-known [2]. Further research on the mechanisms of cancer formation at the cellular and DNA level is aimed to elucidate the shape of the dose-response curve in the low-dose regime and improve the precision of epidemiological studies.

Geant4 model assessment of macroscopic health dosimetry quantities from exposure to radon

Obtaining dose estimates using CT scans allows for the use of unique, patient-specific geometries. Developed as an open source Monte Carlo particle track-

ing code by CERN, Geant4 has expanded into a multidisciplinary simulation and modeling tool that includes codes and toolkits for medical applications on large and small biological scales. For dose assessment on an organ scale, the Geant4 DICOM code [10] allows the user to input DICOM files that define the simulation geometry. Each DICOM file from a CT scan is a slice of geometry in the *z*-direction and the Hounsfield unit values correspond to tissue densities and materials defined by the user. In the presented radon exposure CT-based model, the material densities are used to form the ICRU 46 report [10]. Source definitions are easily described and modified in a macro file and can be placed in areas of interest by selecting the coordinates in a DICOM viewer.

The set of DICOM files used in this study correspond to the CT scan of an adult person torso. The file structure amounts to 100 slices of 2.5 mm in its thickness. To estimate the macroscopic absorbed or dose equivalent in the lungs due to inhalation of short-lived radon progeny, sources of different types and shapes were placed at the main bronchial bifurcation in DICOM geometry. These short-lived progeny are both alpha and beta emitters, as shown in tab. 1, including: (a) alphas of energies 6.0 MeV and 7.69 MeV (corresponding to the decay energies of ^{218}Po and ^{214}Po), and (b) intermediate beta particles from the decay of ^{214}Pb and ^{214}Bi of energies 0.7117 MeV and 2.13 MeV, respectively. The beta decay energies are calculated as the weighted energy of all beta radioactive decay pathways for ^{214}Pb and ^{214}Bi. Literature provides varying estimates of the contribution of the beta radiation to the total dose [11, 12]. For example, Fakir *et al*. estimate that the contribution of beta and gamma radiation to the absorbed dose is below 1% [12], while Leonard *et al*. estimate the beta contribution to be about 20 % [13]. Source shapes were chosen based on those found in literature (cylindrical) [14], as well as those that most closely approximate the bronchial bifurcation geometry (ellipsoidal) from the CT image. These geometries are approximated based on fig. 1.

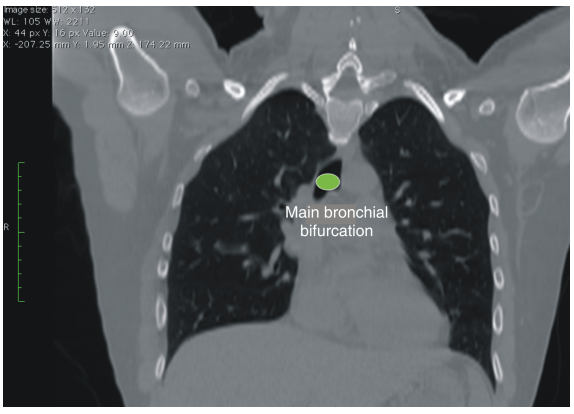

Figure 1. Sagittal view of source region above carinal ridge in main bronchial bifurcation (Osirix), as modeled in Geant4 macroscopic dosimetry model

The source volumes were selected to be spatially homogeneous with ratios of short-lived progeny (^{218}Po, ^{214}Pb, ^{214}Bi, and ^{214}Po), to each other equal to 5:3:2:2 [13]. Additionally, the equilibrium fraction of the progeny to the radon concentration was set to 0.4 [15]. The equilibrium fraction indicates the fraction of radon decay product concentration in relation to the concentration of radon gas. Typical indoor residential equilibrium fractions can vary from location to location, but are usually taken to be ~0.4 [15]. The Geant4 macroscopic model includes 10^8 source particles (such a high number of source particles results in the reduction of error, although error quantification is not provided by Geant4).

To analyze the Geant4 DICOM values, parameters like radon concentration, expected number of disintegrations in the source volume, time of exposure to radon inhalation, and radiation quality factor, must all be combined. A conservative estimate of the dose rate assumes that an individual is exposed to a concentration of ^{222}Rn equal to 148 Bq/m^3 over 18 hours per day per year; thus, the relationship between the Geant4 absorbed dose value in Gy to the equivalent dose rate [mrem per year) is defined as follows

$$\dot{D} \quad D_{\mathrm{A}} N \quad {}^{1}C_{\mathrm{Rn}} F_{\mathrm{E}} F_{\alpha} V Q_{\alpha} \tag{1}$$

where D_{A} is the absorbed dose (Gy), N – the number of source particles, C_{Rn} – the concentration of ^{222}Rn (pCi*/L), F_{E} – the equilibrium fraction of short-lived progeny to ^{222}Rn, F_{α} – the fraction of alpha-emitting progeny, V [m^3] – the source volume, and Q – the quality factor of alpha radiation for equivalent dose calculations (in this study, taken to be 20). For beta particles, the Q is equal to 1.

Geant4 model assessment of nano-dosimetry quantities from exposure to radon

The tendency of the solid decay products of radon to attach to aerosol particles and deposit in bronchial bifurcations leads to higher energy deposition in very small sections of lung tissue [16]. Sensitive targets in the lungs include bronchial epithelial and bronchial secretory cells. To evaluate the dosimetry parameters at this scale, quantities related to particle track structure such as energy deposition, step length, and interaction types along the track are of more interest than the absorbed dose or dose equivalent. To understand these quantities, the simulation of alpha particles of energies corresponding to those of the radon progeny alpha-emitters was created using the Geant4-DNA toolkit and the dnaphysics application[17, 18]. A cube of liquid water of side length 100 m represents a small section of a lung tissue. The general particle source of alphas of energies 6.0 MeV and 7.69 MeV are compared to a range of alpha particle energies

*1 Ci = 3.7 10^{10} Bq

(1 MeV-10 MeV) to evaluate the track structure and resulting particles interactions.

Ionization events are of interest in examining the probability of double-strand breaks (DSB) in the DNA molecule. The ionization events and their positions can be grouped into clusters corresponding to the distance required to induce breaks within the 10-base-pairs in the DNA. The density-based spatial clustering of applications with the noise (DBSCAN) algorithm is applicable since it requires only two parameters: a Euclidean distance and a number of points needed to form a cluster. The *scikit-learn* library contains a DBSCAN routine that was used for this purpose [19]. The DBSCAN algorithm has been successfully used in other Monte Carlo DNA simulations. The number of clusters along the alpha particle track and their probability of interacting with the DNA molecule can be analyzed to estimate the number of DSB candidates expected from the exposure to radon progeny.

RESULTS

Geant4 macroscopic health dosimetry quantities from exposure to radon

The equivalent dose rate from exposure to indoor radon concentration of 148 Bq/m^3 (4 pCi/L) was calculated using patient CT scan data as described in the section *Radon exposure*. The resulting macroscopic equivalent dose values are summarized in tab. 2. The fractional concentration of alpha emitters is 35.9 Bq/m^3 and the fractional concentration of beta emitters is 24.8 Bq/m^3 for an indoor radon concentration of 148 Bq/m^3 and an equilibrium concentration of 0.4 and a 5:3:2:2 ratio of short-lived progeny to each other. As can be seen, the equivalent radiation dose varies only slightly with source shape. The variations in bronchial geometry have an effect on the dose. The expected effective dose rate can be estimated adding the aspects analysis available in literature. The study by Kendall and Smith [11] estimates that a person exposed to a 148 Bq/m^3 (4 pCi/L) concentration of radon would receive an effective dose between 3.18-14.11 mSv per year (318-1411 mrem per year), based on ICRP values of phantom models [11] and not the real human CT-data. In another study by EL-Hussein *et al*. [6], the effective dose rates were found to be between 2.28-6.62 mSv per year (228-662 mrem per year)for the same radon exposure, much closer to the effective doses presented in tab. 2 which were between 0.52--2.31 mSv per year (52-231 mrem per year). The dose rates as shown in tab. 2 fall within the low end of this range when the largest source volumes are used and would correspond to levels of low-dose radiation. The accepted tissue-weighting factor 0.12 was used with the values in tab. 2 to obtain the effective dose values [5]. The dose rates obtained with beta-particle sources represent less than 1 % of those from alpha sources, in agreement with some of the values reported in literature [12].

Table 2. Geant4 CT scan-based macroscopic equivalent doses from alpha and beta particles expressed in [mSv per year] as a function of source shape (cylinder, C, and ellipsoid, E)

Source type and volume [mm^3]	Alphas	Betas
C 817.2	4.36	0.03
E 817.6	4.36	0.03
C 1047.7	5.60	0.04
E 1047.8	5.60	0.04
C 2656.6	14.21	0.09
E 2658.7	19.26	0.09
C 3602.2	19.26	0.12
E 3602.2	19.24	0.12

Geant4 nanodosimetry quantities from exposure to radon

The Geant4-DNA simulations using different energies of alpha particles in the micro-volume of liquid water follow a single alpha particle through a small volume to determine the interactions that occur in a small section of tissue. Geant4 allows for the track structure to be examined for alphas of different energies.

The interactions of the particle and its secondary electrons are stored in n-tuples in ROOT. The most dominant particle type is shown to be from secondary electrons and the most common interaction was electron elastic scattering, as can be seen in fig. 2. ROOT counts each interaction type and bins the results by number. The indicated interactions in fig. 2 are of interest because of their importance in creating double-strand breaks. In each energy category of alphas, ionizations are a dominant interaction, especially, and expectedly, as energy increases.The proximity of these ionizations to each other is also important; the 1992 study by Brenner and Ward showed that multiple ionizations within a site of 2-3 nm in length should "correlate well" to the occurrence of double-strand breaks in the DNA molecule [20].

The ionization events are clustered into groups of three or more within a distance of 3.2 nm of each other. These clusters form DSB candidates. No assumptions are made as to the position of cells or cell nuclei in the simulation tissue volume, so the clustering technique does not distinguish between clustered SSB and clustered DSB. However, the DSB candidates *do* give a conservative estimate of the cellular damage inflicted by ^{222}Rn progeny. The number of cells a particle traverses is calculated using the ranges of the alpha particle in liquid water from ASTAR tables [21]. Table 3 shows these ranges, as well as the number of ionization events asociated with the alpha

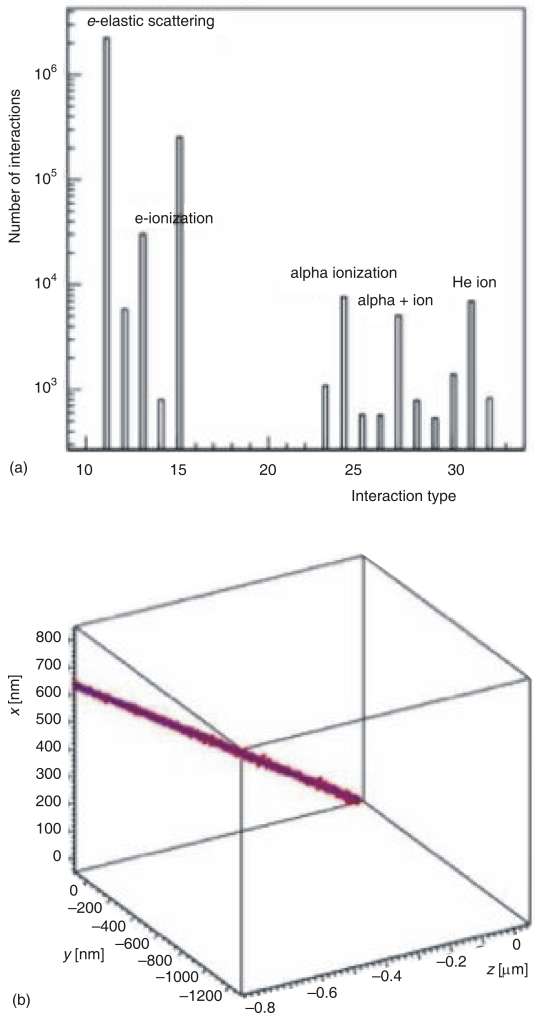

Figure 2. Interaction types (a) and microscopic tissue geometry in Geant4-DNA (b). The interactions are: alpha excitations (23), alpha ionizations (24), alpha charge decrease to $^{+}$ (25), $^{+}$ excitation (26), $^{+}$ ionization (27), $^{+}$ charge decrease to helium (28), $^{+}$ charge increase (29), helium excitation (30), helium ionization (31), and helium charge increase (32)

Table 3. Alpha range in tissue, number of ionization events along path length (from small volume model in Geant4), and number of chosen DBSCAN cluster sizes

Alpha energy [MeV]	ASTAR range in tissue [m]	Geant 4 ionization events	DBSCAN clusters 3.2 nm
1	6	50,104	41
3	18	153,469	200
5	37	256,704	2,019
6	49	307,868	2,525
7.69	73	394,754	3,062
9	95	462,515	3,488
10	113	514,274	3,700

particle track (obtained from Geant4). The DBSCAN algorithm was used to find the number of clusters of size up to 3.2 nm. These clusters form DSB candidates. No assumptions are made as to the position of cells or cell nuclei in the simulation tissue volume, so the clustering technique does not distinguish between clustered SSB and clustered DSB. However, the DSB candidates do give a conservative estimate of the cellular damage inflicted by ^{222}Rn progeny.

As shown in tab. 3, a 6 MeV alpha particle has a range of about 49 m in tissue and it is therefore expected it will traverse about 3 cells of diameter 15 m. The number of clusters along the particle track is divided between the cells which the particle traverses. Then the number of ionization clusters in each cell, N_i, is multiplied by the probability of hitting the nucleus (the nucleus takes about 10 % of the volume of the cell) and the probability of hitting the DNA molecule (the DNA molecule takes about 0.5 % of the nucleus [22]:

$$P_{\mathrm{DSB}} \quad P_{\mathrm{nucl}} P_{\mathrm{DNA}} \tag{2}$$

This probability is useful when linking the macro CT scan model to the cellular effects of ^{222}Rn progeny exposure. Table 4 shows the results of the probability of DNA molecule hits for each cell traversed by an alpha particle associated with ^{218}Po or ^{214}Po.

Table 4. DNA molecule hits per cell traversed by alpha particles of energies associated with short-lived radon progeny

Alpha energy [MeV]	Cells traversed	Ionization clusters per cell	DNA hits per cell
6	3	842	0.41
7.69	5	612	0.31

For an activity concentration of alpha emitter, [Bqm^{-3}], source volume, V_S, and a cell cycle of t_{cell} in days, the number of alpha-emitting particles deposited N_{dep} can be estimated with

$$N_{\mathrm{dep}} \quad C_{\mathrm{Rn}} F_{\mathrm{E}} F_a V_{\mathrm{S}} \tag{3}$$

Using the probability of DNA hits by an ionization cluster (given in tab. 4), the number of cells traversed by each alpha particle, and N_{dep}, an estimate can be made of the number of DSB that occur in the tissue during a cell cycle

$$N_{\mathrm{DSB}} \quad N_{\mathrm{dep}} N_{\mathrm{traversed}} P_{\mathrm{DSB}} \tag{4}$$

Using the same activity concentration of 148 Bq/m^3 (as used in the CT scan model), an exposure time of 18 hours per day, and cell cycle time 30 days, the approximate number of DSB in the main bronchial bifurcation are calculated for the two largest volumes from the CT scan Geant4 model. These are listed in tab. 5. To compare the results for different alpha energies, the DNA damage over different energies was plotted in fig. 3. These are compared to the Dos Santos [22] studies and found to be about an order or two lower. However, these studies made use of explicit geometries with respect to cell structure and DNA density. The DNA density

Table 5. Number of DSB associated with alpha-emitter deposition in the main bronchial bifurcation

Alpha particle energy [MeV]	N_{DSB} [V_S = 2,657 mm^3]	N_{DSB} [V_S = 3,602 mm^3]
6	127	173
7.69	51	69
Total DSB per cell cycle	178	242

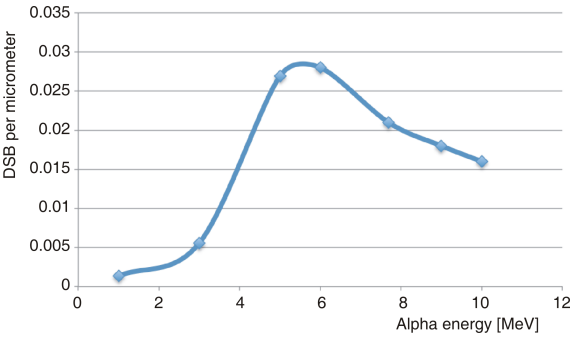

Figure 3. DSB damages (DSB per micrometer) for alpha energies of interest

used here was about three times smaller than the largest one used in studies by Dos Santos.

CONCLUSIONS

In this paper we presented two Geant4 models developed to assess the dose rates, particle track structures, and DNA damages associated with low-dose exposure to indoor radon.

The macroscopic Geant4 model is based on CT scan DICOM data providing patient-specific geometries to estimate how the short-lived progeny of radon deposit dose in the main bronchial bifurcation. The simulation results (using the largest source volumes) were in the range spanning examples in literature to those expected for exposure to radon concentrations at the EPA-recommended action level of 148 Bq/m^3 (4 pCi/L) (about 2.3 mSv per year or 230 mrem per year) [23]. This model makes use of unique geometries and further work may include respiratory dynamics, aerosol attachment, and other biological parameters. The ability to correlate dose rates and biological effects to indoor radon activity concentrations could assist medical professionals in patient treatments, as well as strengthen the predictions made in epidemiological studies.

Since the mechanisms of cancer formation are not well known, nanodosimetric quantities are an important component of the study. Based on the microscopic Geant4 model, the alpha particle track structures were examined and ionization events clustered using a DBSCAN algorithm [19]. The clusters were used to estimate the probability of an alpha-emitter causing a double-strand break in the DNA molecule. Although the geometry of the Geant4-DNA model is simple and the clustering algorithm does not distinguish between clustered single-strand and double-strand breaks, this does offer an estimate for the number of DSBs expected in the tissue of a person exposed to a particular concentration of indoor ^{222}Rn. The estimates were lower than those found in similar studies (but not based on Geant4), indicating that very detailed cell structure geometries offer more insight into the type of physical damage inflicted by ionizing radiation on the DNA molecule.

Lastly, this study showed that the Geant4 code is well suitable for medical-based studies at macroscopic and microscopic levels.

ACKNOWLEDGEMENT

This research is funded by The Nuclear Regulatory Commission Fellowship Program, 2013-2015.

AUTHOR CONTRIBUTIONS

The idea of developing a macroscopic and microscopic analysis of radon exposure using Geant4 was conceived by T. Jevremovic. Simulation models were done by M. van den Akker and M. Lund. The simulation data were interpreted and analyzed by M. van den Akker. All authors contributed to the final conclusions reached.

REFERENCES

[1] Turner, M., *et al.*, Radon and Lung Cancer in the American Cancer Society Cohort, *Cancer Epidemiol Biomarkers Prev., 20* (2011), 3, pp. 438-448
[2] Salomaa, S., *et al.*, State-of-the-Art Research into the Risk of Low Dose Radiation Exposure-Findings of the fourth MELODI Workshop, *J. Radiol. Prot., 33* (2013), 3, pp. 589-603
[3] Goodhead, D. T., Understanding and Characterisation of the Risks to Human Health from Exposure to Low Levels of radiation, *Radiat. Prot. Dosim., 137* (2009), pp. 271-350
[4] Sonzogni, A., Interactive Chart of Nuclides: NuDat 2.6. http://www.nndc.bnl.gov/nudat2 (accessed February 28, 2105)
[5] Turner, J. E., Atoms, Radiation, and Radiation Protection, 3rd ed.; John Wiley and Sons, Germany, 2007
[6] El-Hussein, A., Ahmed, A. A., Mohammed, A., Radiation Dose to the Human Respiratory Tract from Inhalation of Rn-222 and its Progeny, *Appl. Radiat. Isot., 49* (1998), 7, pp. 783-790
[7] Ruzer, L. S., Measurement, Dosimetry, and Health Effects, in: Aerosols Handbook, 2nd ed., Eds.: L. S., Ruzer, N. H. Harley, Taylor & Francis, Boca Raton, Fla., USA, 2012, pp. 383-412
[8] Monson, R. R., *et al.*, Report in Brief: BEIR VII: Health Risks from Exposure to Low Levels of Ionizing Radiation, National Research Council, Washington, D. C., 2005

[9] Zeeb, H., Shannoun, F., WHO hand book on indoor radon:A public health perspective, World Health Organization, Geneva, Switzerland, 2010
[10] Archambault, L., Beaulieu, L., Hubert-Tremblay, V., DICOM example, http://geant4.web.cern.ch/geant4/UserDocumentation/Doxygen/examples_doc/html/ExampleDICOM.html, 2013
[11] Kendall, G. M., Smith, T. J., Doses to Organs and Tissues from Radon and its Decay Products, *J. Radiol. Prot., 22* (2002), 4, pp. 389-406
[12] Fakir, H., *et al*., Microdosimetry of Inhomogeneous Radon Progeny Distributions in Bronchial Airways, *Radiat. Prot. Dosim., 113* (2005), 2, pp. 129-139
[13] Leonard, B., Thompson, R., Beecher, G., Human Lung Cancer Risks from Radon, Part II, Influence from Combined Adaptive Response and Bystander Effects, a Microdose Analysis, *Dose-Response, 9* (2011), 4, pp. 502-553
[14] Nikezic, D., Haque, A. K. M. M., Yu, K. N., Absorbed Dose Delivered by Alpha Particles Calculated in Cylindrical Geometry, *J. Environ. Radioactivity, 60* (2002), 3, pp. 293-305
[15] Pawel, D., Puskin, J., EPA Assessment of Risks from Radon in Homes, United States Environmental Protection Agency; EPA 402-R-03-003, 2003
[16] Madas, B. G., Varga, K., Biophysical Modelling of the Effects of Inhaled Radon Progeny on the Bronchial Epithelium for the Estimation of the Relationships Applied in the Two-Stage Clonal Expansion Model of Carcinogenesis, *Radiat. Prot. Dosim., 159* (2014), 1-4, pp. 237-241
[17] Incerti, A., *et al*., Comparison of Geant4 Very Low Energy Cross Section Models with Experimental Data in Water, *Med. Phys., 37* (2010), 9, pp. 4692-4708
[18] Incerti., S., Karamitros, M., Geant4-DNA Dnaphysics Example, http://geant4-dna.org/, 2014
[19] Pedregosa, F., *et al*., Scikit-Learn: Machine Learning in Python, *J. Mach. Learn. Res., 12* (2011), pp. 2825-2830
[20] Nettlebeck, H., Rabus, H., Nanodosimetry: The Missing Link between Radiobiology and Radiation Physics?, *Radiation Measurements, 46* (2011), 9, pp. 893-897
[21] ***, ASTAR: Stopping Power and Range Tables for Helium Ions. http://physics.nist.gov/PhysRefData/Star/Text/ASTAR.html (accessed Jun 1, 2015)
[22] Dos Santos, M., *et al.*, Influence of Chromatin Densityon the Number of Direct Clustered Damages Calculated for Proton and Alpha Irradiations Using a Monte Carlo Code, *Progress in Nuclear Science and Technology, 4* (2014), pp. 449-453
[23] ***, Radiation Doses in Perspsective, U. S. Environmental Protection Agency, http://www.epa.gov/radiation/understand/perspective.html, (accessed February 27, 2015).

Received on August 24, 2015
Accepted on September 14, 2015

Евелин ВАН ДЕН АКЕР, Метју ЛУНД, Татјана ЈЕВРЕМОВИЋ

ПРОЦЕНА ДОЗИМЕТРИЈСКИХ ПАРАМЕТАРА РАДОНА НА ОСНОВУ Geant4 СИМУЛАЦИЈА И КОРИШЋЕЊА КОМПЈУТЕРИЗОВАНЕ ТОМОГРАФИЈЕ И ЋЕЛИЈСКОГ МОДЕЛА

Процена здравствених ефеката акумулације радона у плућима од значаја је имајући у виду да је радон после пушења други најважнији фактор који изазива канцер. Корелација између дозе зрачења и појаве канцера није довољно објашњена у домену ниских доза, то јест, у опсегу доза акумулације радона. Зато су истраживања у овој области од значаја, нарочито покушаји да се анализира праг вредности дозе изнад које је могуће предвидети потенцијалну појаву канцера услед акумулације радона и продуката распада. У овом раду приказан је макроскопски и целуларни нумерички модел процене дозе радона и продуката радиоактивног распада коришћењем Geant4 кода. Макроскопски модел заснован је на реалним подацима компјутеризоване томографије који омогућују моделовање акумулације радона у плућима у најегзактнијим геометријама. Микроскопска анализа дозе радона и продуката распада анализирана је на нивоу ћелије. Овај модел омогућава анализу интеракција продуката радиоактивног распада и јонизационих потенцијала. Резултати ових анализа такође показују да Geant4 омогућује ефектно моделовање дозиметријских параметара услед акумулације радона и продуката распада на макроскопском и ћелијском нивоу.

Кључне речи: дозиметрија, радон, Geant4, компјутеризована томографија